Experimentally Ruling Out Joint Reality Based on Locality with Device-Independent Steering

Shuaining Zhang[1,2,3], Xiang Zhang[2,3,1], Zhiyue Zheng[1*], and Wei Zhang[2,3,1*]

[1]*Beijing Academy of Quantum Information Sciences, Beijing 100193, China*
[2]*Department of Physics and Beijing Key Laboratory of Opto-electronic Functional Materials and Micro-nano Devices, Renmin University of China, Beijing 100872, China*
[3]*Key Laboratory of Quantum State Construction and Manipulation (Ministry of Education), Renmin University of China, Beijing 100872, China*

(Received 23 November 2023; accepted manuscript online 14 December 2023)

As an essential concept to understand the world, whether the real values (or physical realities) of observables are suitable to physical systems beyond the classic has been debated for many decades. Although standard no-go results based on Bell inequalities have ruled out the joint reality of incompatible quantum observables, the possibility of giving simple yet strong arguments to rule out joint reality in any physical system (not necessarily quantum) with weaker assumptions and less observables has been explored and proposed recently. Here, we perform a device-independent experiment on a two-qubit superconducting system to show that the joint reality of two observables is incompatible with locality under the weaker assumption of the reality of observables in a single space-time region (or single qubit). Our results clearly show the violation of certain inequalities derived from both linear and nonlinear criteria. In addition, we study the robustness of the linear and nonlinear criterion against the effect of systematic decoherence. Our demonstration opens up the possibility of delineating classical and non-classical boundaries with simpler nontrivial quantum system.

DOI: 10.1088/0256-307X/41/1/010301

Observables of a classical system usually admit physical reality (or value definiteness), i.e., the observables have preexisting values when the physical system acts with corresponding measurement procedures. Over the past century, the development of quantum mechanics provides us with a new quantitative description of the microscopic world. The question of whether the physical reality can act on quantum observables was naturally raised by Einstein, Podolsky, and Rosen in 1935,[1] and has been debated for many decades. Thereafter, various no-go results derived under certain assumptions were formulated as inequalities to test the joint reality of incompatible observables. Particularly, the Bell inequalities[2,3] with assumptions of locality and Kochen–Specker (KS) theorems[4,5] with assumptions of measurement noncontextuality are well known and have been verified in many physical experiments.[6–17]

Although the existing no-go arguments have successfully ruled out joint reality of incompatible quantum observables, they usually require quite strong assumptions such as locality and noncontextuality, apply measurements on three or more observables, or rely on the particular preparations and measurements of the quantum device. Distinctive examples include the no-go theorems based on Bell inequalities[2,3,6–9] and Kochen–Specker arguments,[4,5,10–13,18–20] as well as generalized measurement noncontextuality,[14,15,21–23] where measurements are operationally equivalent and cannot be distinguished by the statistics for any preparation. The possibility of ruling out joint reality under weaker assumptions and even less observables with device-independent arguments that can be applied to any physical systems (not necessarily described by quantum mechanics), is still a fundamental question to explore.

Here, we focus on some arguments that can rule out the joint reality of two incompatible observables of a physical system, and introduce two simple yet strong no-go theorems with weaker assumption than those demonstrated previously. The first one is a device-independent steering linear inequality to show the incompatibility of joint reality and locality[24] with the assumption that the reality of observables is only hypothetical in a single space-time region, which is weaker than the standard Bell nonlocality scenario. The second one is a nonlinear inequality derived under preparation noncontextuality where preparations are operationally equivalent correspond to the same state mixtures and cannot be distinguished by any observed statistics results. Then we use a two-qubit superconducting system to perform the two device-independent no-go tests, and observe significant violations of both inequalities, i.e., we experimentally rule out the possibility that two incompatible observables can have real prede-

*Corresponding author. Email: zhengzy@baqis.ac.cn; wzhangl@ruc.edu.cn
© 2024 Chinese Physical Society and IOP Publishing Ltd

termined values in our setup, which can quantify the nonclassicality of a physical system. Moreover, by introducing the effect of systematic decoherence, we study the robustness of the two criterions and find out the nonlinear criterion is more robust against the systematic decoherence.

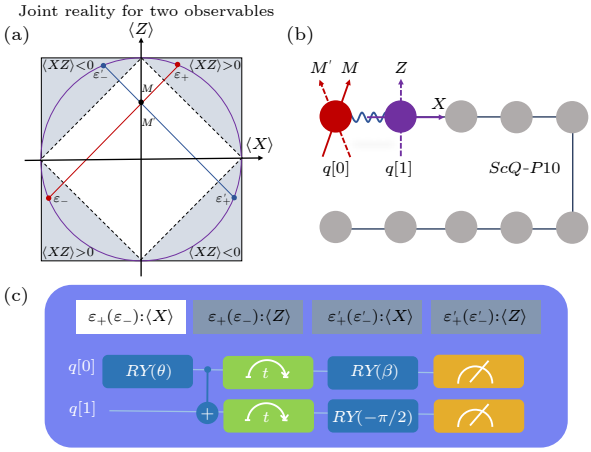

Fig. 1. (a) The joint reality vs locality for two observables X and Z from geometry. This particular case is corresponding to the justification and derivation of Eq. (1) for $c = 0$. The disk $\langle X\rangle^2 + \langle Z\rangle^2 \leq 1$ (purple solid curve) is restricted by quantum mechanics. The red and blue dots depict four ensembles $\{\varepsilon_\pm, \varepsilon'_\pm\}$ that are collapsed from the spin measurement M and M' on one qubit of two-qubit entanglement (or singlet) state. The observations of joint reality from geometry give $\langle XZ\rangle_\varepsilon > 0$ and $\langle XZ\rangle_{\varepsilon'} < 0$. The incompatible result $\langle XZ\rangle_\varepsilon = \langle XZ\rangle_{\varepsilon'}$ can be derived from locality. (b) The system setup. The qubit $q[0]$ and $q[1]$ of *ScQ-P10* superconducting system in the *Cloud* of the Internet are used to implement our protocol. The spin measurements along M and M' bases are applied on $q[0]$ and the measurements of average value for observables X and Z are obtained on $q[1]$. (c) The experimental sequence for measuring $\langle X\rangle_{\varepsilon_+}$ and $\langle X\rangle_{\varepsilon_-}$. $RY(\theta)$ is the single-qubit rotation along Y axis with angle θ, and the green block is a delay with time t.

We consider two observables of a physical system (not necessarily quantum) having joint reality if their measurement outcomes possess preexisting values such as α, $\beta = \pm 1$, respectively. Here, the two observables can be any two-valued observables of any physical system, indicating that the scenario is device-independent. For simplification, we use spin observables X and Z of the qubit system as an example to demonstrate the no-go theorems, where $X = \sigma_x$ and $Z = \sigma_z$ are Pauli operators, as shown in Fig. 1(a). For an ensemble of such a quantum system, the average value of $\langle XZ\rangle$ can be well-defined by relative frequencies $N(\alpha, \beta)/N$, where $N(\alpha, \beta)$ is the number of obtaining $X = \alpha$, $Z = \beta$ when performing the standard quantum probabilistic measurement procedure. The definition is similar for the average values of $\langle X\rangle$ and $\langle Z\rangle$. It can be simply observed that if both $\langle X\rangle$ and $\langle Z\rangle$ are sufficiently positive, $\langle XZ\rangle$ would be conclusively positive, as shown in the upper right shaded region (restricted by quantum mechanics with the purple carve) in Fig. 1(a), that is,

$$\langle XZ\rangle > 0, \quad \text{for} \quad \langle X\rangle + \langle Z\rangle > 1.$$

This result can also be directly obtained by the positivity of relative frequencies as $N(\alpha, \beta)/N = [1+\alpha\langle X\rangle+\beta\langle Z\rangle+\alpha\beta\langle XZ\rangle]/4 \geq 0$. Naturally, we get $\langle XZ\rangle_{\varepsilon_+} > 0$ for an ensemble state ε_+ of the system, corresponding to the red dot in the upper right region.

Similarly, one can see

$$\begin{aligned}
&\langle XZ\rangle > 0, \quad \text{for} \quad \langle X\rangle + \langle Z\rangle < -1,\\
&\langle XZ\rangle < 0, \quad \text{for} \quad \langle X\rangle - \langle Z\rangle > 1,\\
&\langle XZ\rangle < 0, \quad \text{for} \quad \langle X\rangle - \langle Z\rangle < -1,
\end{aligned}$$

and the observations $\langle XZ\rangle_{\varepsilon_-} > 0$, $\langle XZ\rangle_{\varepsilon'_+} < 0$, and $\langle XZ\rangle_{\varepsilon'_-} < 0$ for ensembles ε_-, ε'_+, and ε'_-, corresponding to the red and blue dots in the lower left, lower right, and upper left regions, can be easily obtained. Then, the average value of $\langle XZ\rangle$ for the mixture ensemble ε of two sub-ensembles ε_+ and ε_- would also be determined as $\langle XZ\rangle_\varepsilon > 0$. Similarly, we get $\langle XZ\rangle_{\varepsilon'} < 0$. These observations are determined by the joint reality of two observables X and Z based on the classical geometry.

In the quantum system, the above scenario can be designed to happen and tested in the measurement procedure of a certain two-qubit entanglement (or singlet) state. A spin measurement on the first qubit in the M basis [the red line in Fig. 1(a)] would collapse the state ensemble to the mixture ensemble ε, then the spin measurement on the second qubit could obtain the average value $\langle XZ\rangle_\varepsilon$. Similarly, a spin measurement on the first qubit in the M' basis (the blue line) would collapse the state ensemble to mixture ε' and then $\langle XZ\rangle_{\varepsilon'}$ can be also measured. If one considers the assumption of locality that the real values of X and Z on the second qubit should be independent of which measurement is applied to the first qubit, the measurement result for $\langle XZ\rangle$ on the mixture ensemble ε and ε' would be $\langle XZ\rangle_\varepsilon = \langle XZ\rangle_{\varepsilon'}$, which is incompatible with the observations of the joint reality of X and Z from geometry. Note that this result does not assume any reality on the first qubit, which is here called the single space-time reality assumption and is weaker than the standard Bell nonlocality scenario.

Then, we introduce the first no-go theorem derived from the above descriptions that the joint reality of the two observables X and Z on one qubit is compatible with locality only if the inequality [24]

$$\begin{aligned}
\ell_c = \min\big\{&\langle X\rangle_{\varepsilon_+} + \langle Z\rangle_{\varepsilon_+} - 1 - c,\\
&-\langle X\rangle_{\varepsilon_-} - \langle Z\rangle_{\varepsilon_-} - 1 - c,\\
&\langle X\rangle_{\varepsilon'_+} - \langle Z\rangle_{\varepsilon'_+} - 1 + c,\\
&-\langle X\rangle_{\varepsilon'_-} + \langle Z\rangle_{\varepsilon'_-} - 1 + c\big\} \leq 0
\end{aligned} \tag{1}$$

holds for sub-ensembles $\{\varepsilon_\pm, \varepsilon'_\pm\}$ corresponding to the measurement M and M' applied on the other qubit, where

$c \in (-1, 1)$. The parameter c is introduced to make the theorem suitable for general and arbitrary qubit observables, which reduces to the situation in Fig. 1(a) when $c = 0$. The other nonlinear no-go theorem [24] can be obtained based on preparation noncontextuality [25] as

$$\tau = \begin{vmatrix} \langle X\rangle_{\varepsilon_+} & \langle Z\rangle_{\varepsilon_+} & p\langle X\rangle_{\varepsilon_+} + q\langle Z\rangle_{\varepsilon_+} - 1 & 1 \\ \langle X\rangle_{\varepsilon'_+} & \langle Z\rangle_{\varepsilon'_+} & r\langle X\rangle_{\varepsilon'_+} + s\langle Z\rangle_{\varepsilon'_+} + 1 & 1 \\ \langle X\rangle_{\varepsilon'_-} & \langle Z\rangle_{\varepsilon'_-} & -r\langle X\rangle_{\varepsilon'_-} - s\langle Z\rangle_{\varepsilon'_-} + 1 & 1 \\ \langle X\rangle_{\varepsilon_-} & \langle Z\rangle_{\varepsilon_-} & -p\langle X\rangle_{\varepsilon_-} - q\langle Z\rangle_{\varepsilon_-} - 1 & 1 \end{vmatrix} \leq 0 \tag{2}$$

for all p, q, r, $s = \pm 1$ with $pqrs = -1$.

We can use a two-qubit system to test the above two no-go theorems. The computation basis of a single qubit is defined as $\{|0\rangle, |1\rangle\}$. The protocol is as follows: First, prepare an entanglement state

$$|\psi\rangle = \cos(\theta)|00\rangle + \sin(\theta)|11\rangle, \theta \in (0, \pi/2). \tag{3}$$

Then, perform spin measurements on the first qubit along basis

$$M = \frac{\sin(2\theta)}{\sqrt{1+\sin^2(2\theta)}}X + \frac{1}{\sqrt{1+\sin^2(2\theta)}}Z$$

or

$$M' = \frac{\sin(2\theta)}{\sqrt{1+\sin^2(2\theta)}}X - \frac{1}{\sqrt{1+\sin^2(2\theta)}}Z.$$

After applying measurement on the first qubit, the second qubit would collapse to one of the four ensembles $\{\varepsilon_\pm, \varepsilon'_\pm\}$ with the corresponding probabilities; finally, through spin measurement on the second qubit along bases X and Z, we can obtain the average value of the two observables on the four ensembles, which is exactly required for testing the two no-go arguments. When $\theta = \pi/4$, the maximal violation is $\ell_{\max} = \sqrt{2} - 1 \approx 0.414$ and $\tau_{\max} = 8(\sqrt{2} - 1) \approx 3.314$, respectively. Here, we intentionally choose $\theta = \pi/6$ corresponding to the situation in Fig. 1(a), to study the effect of the two inequalities against systematic decoherence, which leads to $\ell_{\max} = (\sqrt{7} - 2)/2 \approx 0.323$ and $\tau_{\max} = 7(\sqrt{7} - 2)/2 \approx 2.260$.

To experimentally implement the above protocol, we introduce the *Quafu* superconducting system at the Beijing Academy of Quantum Information Science (BAQIS), which is accessible in the *Cloud* of the Internet. We choose the chip *ScQ-P10* as the platform to run our circuits, as shown in Fig. 1(b). *ScQ-P10* contains ten qubits and has an average depopulation time $T_1 = 33.712\,\mu s$ and decoherence time $T_2 = 2.128\,\mu s$. One can program and implement the standard quantum circuits composed of single- and two-qubit gates with it. The gate time is 40 ns and gate fidelity is 99.1% at maximum.

We choose two qubits out of ten on the chip *ScQ-P10* and encode the first qubit $q[0]$ as the ancillary qubit to perform spin measurement on bases M and M' for collapsing the system to the desired ensembles $\{\varepsilon_\pm, \varepsilon'_\pm\}$, and then perform the measurement of observables X and Z on the second qubit $q[1]$. The experimental sequence is shown in Fig. 1(c). Taking the measurement of $\langle X\rangle_{\varepsilon_+}$ and $\langle X\rangle_{\varepsilon_-}$ as an example: First, we apply a single-qubit rotation along Y axis as $RY(\theta)$ on $q[0]$ followed by a *cnot* gate to prepare the two-qubit entanglement state in Eq. (3). Then, by adding the delay with time t, we introduce the systematic decoherence. Here, to test the maximal violation of the no-go theorems, we set $t = 0$. A spin measurement along basis M realized by the operation $RY(\beta)$ to rotate the measurement basis from Z to M would make the system collapse to ensemble ε_+ or ε_-, where $\beta = -\arctan(\sin(2\theta))$. Finally, the average (or expectation) values of X and Z can be obtained by spin measurement on $q[1]$. The operation $RY(-\pi/2)$ on $q[1]$ is to rotate the measurement basis from Z to X. In practice, we use the *Python* programming language to run the circuit online. Except for initialization and compilation, the main core code is as follows:

$$\begin{aligned} &q = QuantumCircuit(2) \\ &q.ry(0,\ 2 * np.pi/6) \\ &q.cnot(0,\ 1) \\ &q.delay(0,\ 0,\ unit = \text{“ns”}) \\ &q.delay(1,\ 0,\ unit = \text{“ns”}) \\ &q.ry(0,\ -np.\arctan(np.\sin(2 * np.pi/6))) \\ &q.ry(1,\ -np.pi/2) \\ &measures = [0,\ 1] \\ &cbits = [0,\ 1] \\ &q.measure(measures,\ cbits = cbits) \end{aligned}$$

with package support as “*from quafu import QuantumCircuit*” and “*import numpy as np*”.

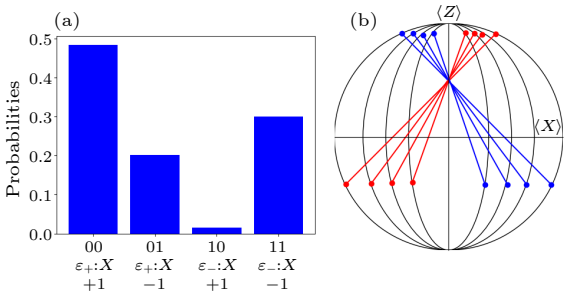

Fig. 2. (a) The measured population distribution of the running circuit in Fig. 1(c). We map the population $|00\rangle$ as the outcome with $+1$ when measuring the observable X on ensemble ε_+, and $|01\rangle$ for the outcome with -1. Combining the population of $|00\rangle$ and $|01\rangle$, we can calculate the average value of X on ensemble ε_+, labeled as $\langle X\rangle_{\varepsilon_+}$. Similarly, $\langle X\rangle_{\varepsilon_-}$ is obtained based on the population of $|10\rangle$ and $|11\rangle$. (b) The positions of the measured average values of X and Z for different ensembles on the X–Z plane. By changing the delay time with $t \approx 0$, 200, 330, 450 ns in Fig. 1(c), we obtain four groups of results that are located on the corresponding circle or elliptic from the outer to inner. The fitted dephasing parameters are $p \approx 0.25$, 0.45, 0.65 for the three elliptics.

Noting that after running the circuit in Fig. 1(c),

the typical result is the population distribution of the four product states with $|00\rangle$, $|01\rangle$, $|10\rangle$, $|11\rangle$, as shown in Fig. 2(a). To obtain the desired average value of X, we map the state $|00\rangle$ to be the outcome with $+1$ when measuring X on ensemble ε_+. Similarly, the state $|01\rangle$ corresponds to the outcome with -1 when measuring X on ensemble ε_+. Then we can recalculate the average value $\langle X\rangle_{\varepsilon_+}$ from the outcome frequency of values with $+1$ and -1. Naturally, the states $|10\rangle$ and $|11\rangle$ are corresponding to the system collapsing to ensemble ε_-, and the average value $\langle X\rangle_{\varepsilon_-}$ is obtained with a similar method. By changing the measurement basis from X to Z on $q[1]$, we also get the average values $\langle Z\rangle_{\varepsilon_+}$ and $\langle Z\rangle_{\varepsilon_-}$. Then, to obtain the results on ensembles ε'_+ and ε'_-, we perform spin measurement on $q[0]$ along the M' basis by changing $\beta = \arctan(\sin(2\theta)) - \pi$, to make the system collapse to the ε'_+ and ε'_-. Through the same mapping, we obtain the average value $\langle X\rangle_{\varepsilon'_+}$, $\langle X\rangle_{\varepsilon'_-}$, $\langle Z\rangle_{\varepsilon'_+}$, and $\langle Z\rangle_{\varepsilon'_-}$.

Now, we have all the measurements of observables X and Z to calculate the maximal violation of the two no-go theorems, assuming that the system has no desired decoherence corresponding to the delay time $t = 0$. From the inequalities (1) and (2), we get $\ell_{\max} = 0.318 \pm 0.017$ and $\tau_{\max} = 2.221 \pm 0.135$, which agree well with the theoretical prediction. Then, we would study the effect of systematic decoherence to the violation of no-go theorems. Considering the decoherence time of the system to be $T_2 = 2.128\,\mu$s, we choose several delay times as $t \approx 200$, 330, 450 ns to run the same sequence, and obtain the required average values for observables X and Z. All the results are shown in Fig. 2(b) with the corresponding red and blue dots.

To quantify the dependence of the violation of no-go theorems on the systematic decoherence, we theoretically simulate the decoherence process and fit our experimental data to a dephasing model. For a single-qubit system, the systematic decoherence interacting with the environment can be approximately treated as a dephasing channel,

$$\Lambda_p(\rho) = \left(1 - \frac{p}{2}\right)\rho + \frac{p}{2} Z\,\rho\, Z, \tag{4}$$

where ρ is the density matrix of the input state, $Z = \sigma_z$ is the Pauli operator, and p is a quantity that describes the contraction ratio of the Bloch sphere on the X–Y plane. Although it is two-qubit decoherence process in our experiment, we can simplify it by contributing the two-qubit decoherence to the effective single-qubit one applied on the ensembles $\{\varepsilon_\pm, \varepsilon'_\pm\}$, which results in the double dephasing parameter p. In the experiment, by increasing the delay time t, we obtain the corresponding average value $\langle X\rangle$ and $\langle Z\rangle$, and the points on the X–Z plane will be located on different elliptical curves, as shown in Fig. 2(b). By fitting points to Eq. (4), we obtain the approximate dephasing parameters with the corresponding delay time as $p \approx 0.25$, 0.45, 0.65.

All the final results of the two no-go theorem tests are shown in Fig. 3, where the solid (blue) and dashed (red) lines are the numerical simulations of the inequalities (1) and (2) as functions of dephasing parameter p, respectively. The blue and red dots are the corresponding experimental results, which agree well with the simulation. Moreover, one can clearly see that the nonlinear inequality (2) is more robust to the systematic decoherence compared with linear inequality (1), which means that for a larger dephasing parameter, the nonlinear inequality can still be violated, rather than the linear inequality. Specifically, the linear inequality (1) is violated only in the regime of $p < 3 - \sqrt{7} \approx 0.354$, in which all the four state ensembles always lie in the shaded region in Fig. 1(a) and the strictly required geometry argument for the linear criteria is fulfilled. In the regime of $p \in (3 - \sqrt{7}, (7 - 2\sqrt{7})/3)$, the nonlinear inequality is still violated because it is derived based on preparation noncontextuality, which focuses on the quantum property of the system itself, rather than the geometry argument. For the regime of $p > (7 - 2\sqrt{7})/3 \approx 0.569$, the system dephases to a chaos situation, in which one cannot observe the difference of a classical and non-classical physical system with the joint reality of two observables.

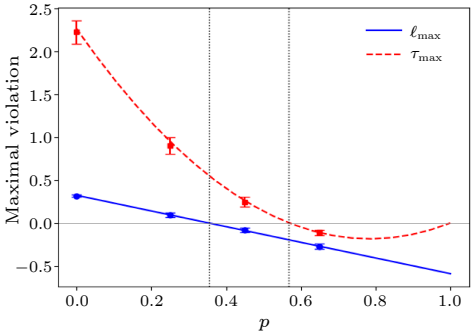

Fig. 3. The maximum violation of the two no-go inequalities versus dephasing parameter p. The solid (blue) and dashed (red) lines are the numerical simulation of the linear and nonlinear inequalities versus dephasing parameter p. The blue and red dots are the corresponding experimental data, which agree well with the numerical simulation. Each piece of data is obtained by running the desired quantum circuits 3000 times. The error bar is one standard deviation of 1000 samples generated from the raw experimental data, using the bootstrapping method. The theoretical thresholds from simulation for the two inequalities are $p = 3 - \sqrt{7} \approx 0.354$ and $p = (7 - 2\sqrt{7})/3 \approx 0.569$, respectively, which are depicted by vertical dotted lines.

In conclusion, we demonstrate device-independent experimental no-go tests of joint reality of two observables on a two-qubit superconducting system. The results show that the joint reality of two observables is incompatible with locality, even under the weaker assumption that the reality of observables is only required in a single space-time region (single qubit), rather than two space-time regions in the standard Bell nonlocality scenario. We clearly observe significant violations of the two inequalities and achieve good agreement with the theoretical prediction. The main error sources in our experiments are the gate

infidelity (0.9% at minimum) and the fluctuated different decoherence time on the two qubits. Then, by introducing the effect of systematic decoherence, we study the robustness of the linear and nonlinear criterion, and find out the nonlinear form is more robust against decoherence. Our work provides a new prospect to understand the classical and non-classical physical system, and inspire the application of noise effects in quantum technology.

Acknowledgments. This work was supported by the National Natural Science Foundation of China (Grant Nos. 12074427, 12074428, 12204535, and 92265208), and the National Key R&D Program of China (Grant Nos. 2018YFA0306501 and 2022YFA1405301). We also acknowledge support from the Quafu cloud platform for quantum computation (https://quafu.baqis.ac.cn/) and the Extreme Condition User Facility in Beijing.

References

[1] Einstein A, Podolsky B, and Rosen N 1935 *Phys. Rev.* **47** 777
[2] Bell J S 1964 *Physics* **1** 195
[3] Brunner N, Cavalcanti D, Pironio S, Scarani V, and Wehner S 2014 *Rev. Mod. Phys.* **86** 419
[4] Kochen S and Specker E P 1968 *Indiana Univ. Math. J.* **17** 59
[5] Budroni C, Cabello A, Gühne O, Kleinmann M, and Larsson J Å 2022 *Rev. Mod. Phys.* **94** 045007
[6] Aspect A, Dalibard J, and Roger G 1982 *Phys. Rev. Lett.* **49** 1804
[7] Weihs G, Jennewein T, Simon C, Weinfurter H, and Zeilinger A 1998 *Phys. Rev. Lett.* **81** 5039
[8] Rowe M A, Kielpinski D, Meyer V, Sackett C A, Itano W M, Monroe C, and Wineland D J 2001 *Nature* **409** 791
[9] Gröblacher S, Paterek T, Kaltenbaek R, Brukner Č, Żukowski M, Aspelmeyer M, and Zeilinger A 2007 *Nature* **446** 871
[10] Kirchmair G, Zähringer F, Gerritsma R, Kleinmann M, Gühne O, Cabello A, Blatt R, and Roos C F 2009 *Nature* **460** 494
[11] Zhang X, Um M, Zhang J, An S, Wang Y, Deng D L, Shen C, Duan L M, and Kim K 2013 *Phys. Rev. Lett.* **110** 070401
[12] Leupold F M, Malinowski M, Zhang C, Negnevitsky V, Cabello A, Alonso J, and Home J P 2018 *Phys. Rev. Lett.* **120** 180401
[13] Wang P F, Zhang J H, Luan C Y, Um M, Wang Y, Qiao M, Xie T, Zhang J N, Cabello A, and Kim K 2022 *Sci. Adv.* **8** eabk1660
[14] Mazurek M D, Pusey M F, Kunjwal R, Resch K J, and Spekkens R W 2016 *Nat. Commun.* **7** 11780
[15] Zhan X, Cavalcanti E G, Li J, Bian Z, Zhang Y, Wiseman H M, and Xue P 2017 *Optica* **4** 966
[16] Spekkens R W, Buzacott D H, Keehn A J, Toner B, and Pryde G J 2009 *Phys. Rev. Lett.* **102** 010401
[17] Mazurek M D, Pusey M F, Resch K J, and Spekkens R W 2021 *PRX Quantum* **2** 020302
[18] Klyachko A A, Can M A, Binicioğlu S, and Shumovsky A S 2008 *Phys. Rev. Lett.* **101** 020403
[19] Yu S X and Oh C H 2012 *Phys. Rev. Lett.* **108** 030402
[20] Kleinmann M, Budroni C, Larsson J Å, Gühne O, and Cabello A 2012 *Phys. Rev. Lett.* **109** 250402
[21] Cabello A 2003 *Phys. Rev. Lett.* **90** 190401
[22] Spekkens R W 2005 *Phys. Rev. A* **71** 052108
[23] Liang Y C, Spekkens R W, and Wiseman H M 2011 *Phys. Rep.* **506** 1
[24] Hall M J W and Rivas Á 2019 *Phys. Rev. A* **100** 062105
[25] Pusey M F 2018 *Phys. Rev. A* **98** 022112